J Mater Sci (2009) 44:3556–3560
DOI 10.1007/s10853-009-3479-7

Thickness effects of $Bi_{3.5}Nd_{0.5}Ti_3O_{12}$ buffer layers on structure and electrical properties of $BiFeO_3$ films

Xuemei Chen · Guangda Hu · Xi Wang · Jing Yan · Changhong Yang · Weibing Wu

Received: 23 October 2008 / Accepted: 8 April 2009 / Published online: 24 April 2009
© Springer Science+Business Media, LLC 2009

Abstract $BiFeO_3$ (BFO) thin films deposited on various thicknesses (0, 40, 80, and 160 nm) of $Bi_{3.5}Nd_{0.5}Ti_3O_{12}$ (BNT) buffer layers were fabricated on indium tin oxide (ITO)/Si substrates using a metal organic decomposition process. X-ray diffraction (XRD) measurements reveal that the BNT buffer layers can favor the growth of (110)-oriented grains in the BFO films. Well-saturated *P*–*E* hysteresis loops can be obtained in BFO films with BNT buffer layers due to their lower leakage current densities compared with that in BFO film deposited directly on ITO/Si substrate. A remanent polarization (P_r) as large as 70.2 ± 2 μC/cm^2 can be achieved in BFO film with 40-nm-thick BNT buffer layer. Further increase of the buffer layer thickness results in the degradation of the rectangularity of *P*–*E* hysteresis loops, reduction of the P_r value, as well as deterioration of the charge-retaining ability for the double-layered films.

Introduction

Multiferroic materials, combining two or more properties of ferromagnetism, ferroelectricity, and ferroelasticity, have attracted much attention in recent years. Of particular interest is $BiFeO_3$ (BFO), which exhibits simultaneously ferroelectric ordering (Curie temperature $T_C = 850$ °C) and antiferromagnetic ordering (Néel temperature $T_N = 370$ °C) above room temperature [1–4]. More recently, it has been shown that enhanced ferroelectric properties of BFO are intrinsic to the material [5–8], suggesting a deserving environmentally benign substitute for Pb-based ferroelectrics.

However, one of the critical drawbacks of BFO is its high leakage current, owing to that the saturated *P*–*E* hysteresis loops cannot be obtained readily in films prepared using the chemical solution deposition method. It has been demonstrated that the leakage currents of BFO films can be considerably decreased by isovalent-ion substitution at Bi sites by lanthanides [9, 10] and Fe sites by Mn^{3+} and Cr^{3+} [11, 12], respectively. On the other hand, introducing a ferroelectric thin film with lower leakage current to form a double-layered structure (such as BFO/$Pb(Zr_{0.5}Ti_{0.5})O_3$ [13], BFO/$Bi_{3.25}Sm_{0.75}Ti_{2.98}V_{0.02}O_{12}$ [14], BFO/$Bi_{3.25}La_{0.75}Ti_3O_{12}$ [15], and BFO/$Bi_{3.15}Nd_{0.85}Ti_3O_{12}$ [16]) has also been verified as an alternative route to improve the insulating properties of BFO films. Nevertheless, the values of the remnant polarization for these double-layered films are much lower compared with the reported values of BFO films fabricated by chemical solution deposition technique [11, 12, 17]. This may be due to that part of the voltage can be applied on the bottom buffer layer since the buffer layer and BFO layer are in series connection, leading to that the domains in the BFO film cannot be fully switched. Therefore, larger P_r value can be expected in BFO-based double-layered structure with thinner buffer layer. Recently, we have demonstrated that the 40-nm-thick buffer layer can reduce the leakage current and improve the ferroelectric properties of BFO film [18]. To further clarify this issue, we have fabricated BFO films on various thicknesses (0, 40, 80, and 160 nm) of $Bi_{3.5}Nd_{0.5}Ti_3O_{12}$ (BNT) buffer layers. In the present work, we report on the dependence of the structure and electrical properties of BFO films on the thickness of BNT buffer layer. Our results indicate that with the increase of the BNT buffer layer thickness, the remnant polarization

X. Chen · G. Hu (✉) · X. Wang · J. Yan · C. Yang · W. Wu
School of Materials Science and Engineering,
University of Jinan, Jinan 250022, China
e-mail: mse_hugd@ujn.edu.cn

of the double-layered thin film decreases, together with the charge-retaining ability.

Experimental

Both BFO and BNT thin films were fabricated on indium tin oxide (ITO)/Si substrate using a metal organic decomposition process. The preparations of the BNT and BFO precursor solutions have been described in our previous works [18, 19]. Prior to depositing the BFO films, the BNT films with layer thicknesses of about 40, 80, and 160 nm were first deposited on the ITO/Si substrates by spin coating and then crystallized at 600 °C in O_2 atmosphere. Subsequently, the BFO films were spin-coated at 3000 rpm for 30 s on top of the three BNT films, and then baked on a hot plate. Each layer of the film was annealed in a rapid thermal annealing furnace at 525 °C for 2 min in a N_2 atmosphere. This process was repeated several times to obtain the desired thickness. A BFO film without BNT buffer layer was also fabricated for comparison. The final thicknesses of all BFO films are about 570 nm. Au top electrodes were deposited on the films using a sputtering system through a shadow mask with a diameter of 200 μm for electrical measurements.

The crystal structure of the films were characterized by X-ray diffraction (XRD) using a Bruker D8 diffractometer with Cu Kα radiation. The surface morphologies were detected using an atomic force microscope (AFM) working in tapping mode. The thicknesses of the BNT buffer layers and BFO films were measured using a scanning electron microscope (SEM). A standard ferroelectric tester (Precision Pro. Radiant Technologies) was used to investigate the leakage current densities and detailed ferroelectric properties of the films.

Results and discussion

Figure 1a shows the XRD patterns of ITO/Si substrate and BNT buffer layers with various thicknesses. It can be seen that all BNT films show similar polycrystalline structure. With the increase of the BNT buffer layer thickness, the intensities of all the diffraction peaks get strengthened. Figure 1b gives the XRD patterns of the BFO films with various BNT buffer layers thicknesses. As can be seen, single perovskite phase free of impurities was obtained. The diffraction peaks were indexed using the pseudocubic structure. The full widths at half-maximum (FWHMs) of the (110) peak are about 0.15°, indicating that all BFO films are well-crystallized. The BFO film deposited directly on the ITO/Si substrate exhibits a polycrystalline structure. In contrast, the BFO film deposited on the 40-nm-thick

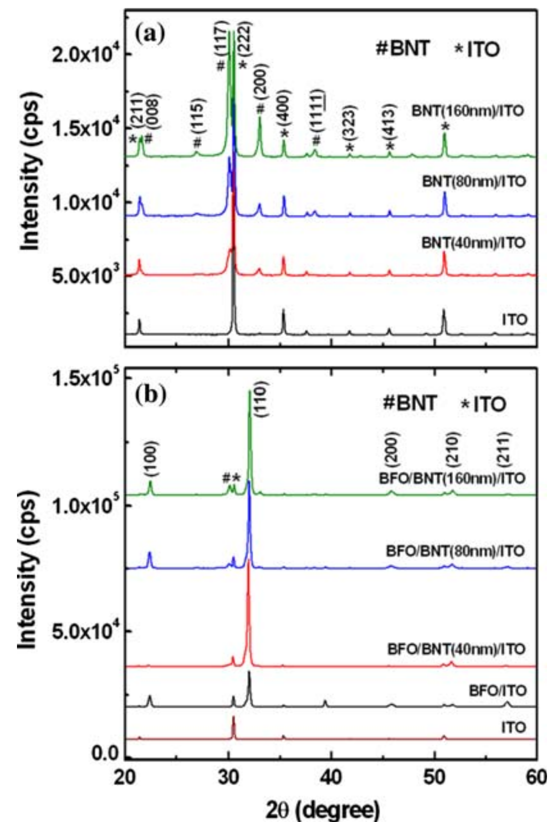

Fig. 1 XRD patterns of **a** ITO/Si substrate and BNT films with the thicknesses of 40, 80, and 160 nm, **b** ITO/Si substrate and BFO films on 0-, 40-, 80-, and 160-nm-thick BNT buffer layers

BNT buffer layer shows the strongest relative intensity of (110) peak and almost undetectable peak of (100). However, further increase of the thickness of the BNT buffer layer results in an evident increase of the relative intensity of (100) peak for BFO film. This phenomenon can be ascribed to the larger grain sizes of the 80- and 160-nm-thick BNT buffer layers (see Fig. 2) as discussed in detail below.

The surface morphologies of ITO/Si substrate and BNT layers with various thicknesses are illustrated in Fig. 2. The root mean square (rms) roughnesses for ITO/Si substrate and 40-, 80-, 160-nm-thick BNT buffer layers are 13.8, 8.2, 9.8, 10.0 nm, respectively. The smaller rms roughness for the 40-nm-thick BNT layer should be due to the highly uniform grain size. One can seen that the 40-nm-thick BNT buffer layer is mainly composed of equiaxed grains about 80 – 140 nm in diameter, while the 80-, 160-nm-thick BNT buffer layers are mainly composed of rod-like grains (grain sizes are around 420 (140 nm)), which has been identified to be (117)-oriented grains [19]. This is consistent with the XRD results of BNT buffer layers. In our previous work, we have reported that there exists epitaxial relationship between the facets of BFO (100) and BNT (001). Since the grain sizes for the 80-, 160-nm-thick BNT

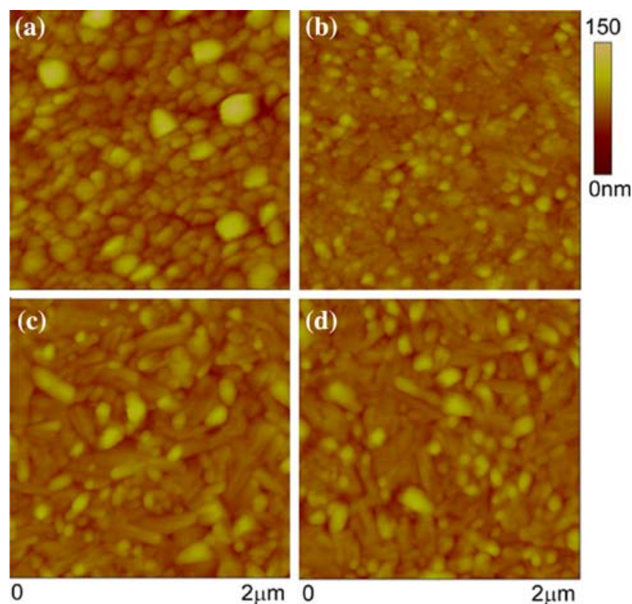

Fig. 2 AFM images of **a** ITO/Si substrate, **b** 40-, **c** 80-, and **d** 160-nm-thick BNT buffer layers

layers are much larger than that for the 40-nm-thick BNT layer, the influence of the epitaxial relationship between the facets of BFO (100) and BNT (001) in the former is much stronger than that in the latter. Therefore, the (100)-oriented grains in BFO films deposited on the 80-, 160-nm-thick BNT layers can not be fully suppressed during the competitive growth with (110)-oriented grains, resulting in the re-emerging of (100) peak in BFO films on 80- and 160-nm-thick BNT buffer layers.

To confirm the thickness and surface morphologies of the BFO films, three-dimensional surface and cross-section scanning were carried out, as shown in Fig. 3. All BFO films are well-crystallized and very dense without any cracks or pin-holes. The rms roughnesses for BFO films with 0-, 40-, 80-, and 160-nm-thick BNT buffer layer are 11.2, 10.6, 11.4, and 11.7 nm, respectively. Note that the grain sizes (150 ± 15 nm) of BFO films with BNT buffer layers are comparable with that of the BFO film deposited directly on ITO/Si substrate, suggesting that the BNT buffer layers do not deteriorate the crystallinity of the top BFO films. From Fig. 3e and f, we can see that the thicknesses of the BNT buffer layers and BFO films are about 40, 160, and 570 nm, respectively.

Figure 4 shows the leakage current density as a function of electric field measured at room temperature. For the BFO films with BNT buffer layers, the breakdown characteristics are much improved in comparison with that for the BFO film deposited directly on ITO/Si substrate. Additionally, the leakage current densities in the former are about one or two orders of magnitude lower than that of the latter, depending on the thickness of the BNT buffer layer.

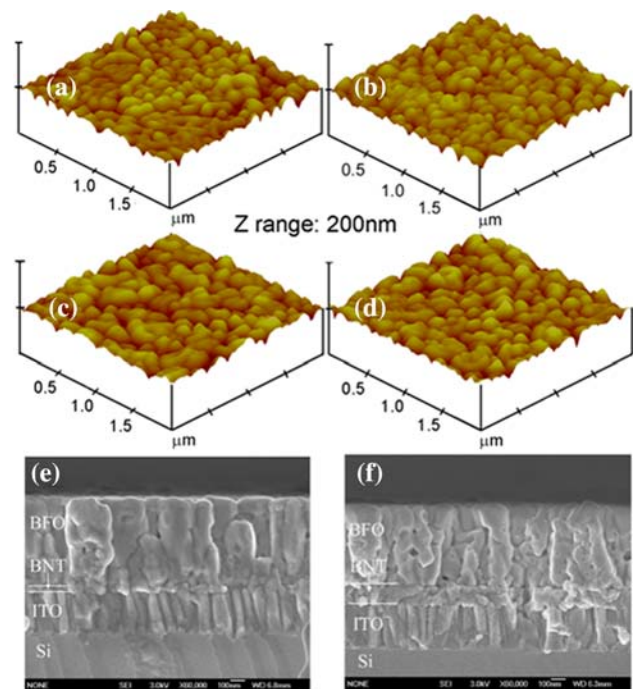

Fig. 3 Three-dimensional AFM images of BFO films on **a** 0-, **b** 40-, **c** 80- and **d** 160-nm-thick BNT buffer layers, as well as cross-sectional SEM images of BFO films on **e** 40- and **f** 160-nm-thick BNT buffer layers

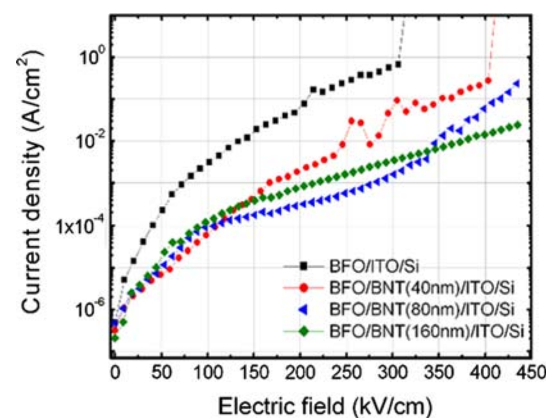

Fig. 4 The Leakage current density as a function of electric field for BFO films on 0-, 40-, 80-, and 160-nm-thick BNT buffer layers

Note that for the electric field higher than 350 kV/cm, the leakage current densities in BFO films with BNT buffer layers decrease slightly with the increase of the buffer layer thickness before breakdown. The lower leakage current densities in BFO films with BNT buffer layers should be due to the good insulating properties of the BNT layers, which can stop charge transfer between BFO film and ITO electrode.

The room temperature hysteresis loops for BFO films with various thicknesses of BNT buffer layers measured at 15 kHz are plotted in Fig. 5. It is worth noting that

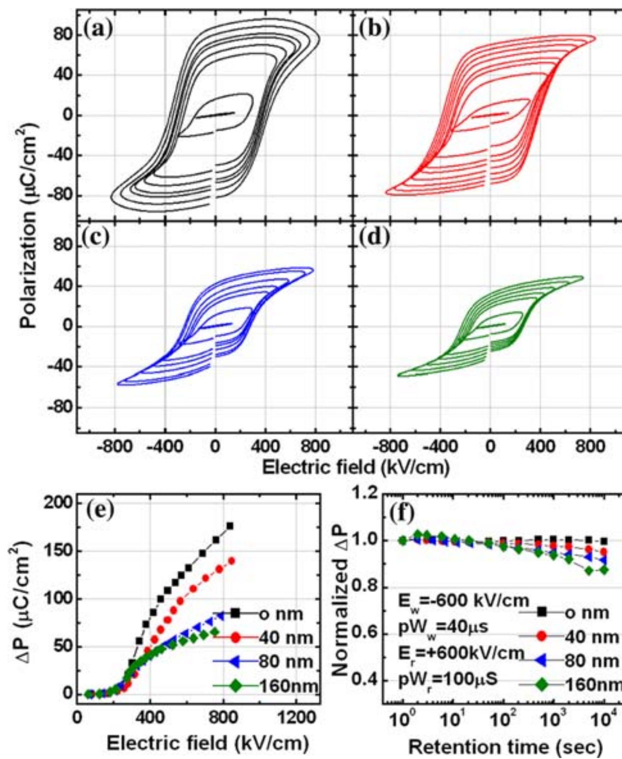

Fig. 5 Room temperature ferroelectric properties for BFO films with different thicknesses of BNT buffer layers. **a–d** *P-E* hysteresis loops for BFO films on 0-, 40-, 80-, and 160-nm-thick BNT buffer layers. **e** The pulsed polarization (ΔP) as a function of electric field. **f** The normalized ΔP as a function of the retention time for all double-layered films

symmetric *P–E* loops can be observed in all samples. Due to the highly leakage nature of the sample, saturated *P–E* loops cannot be observed in the BFO film deposited directly on ITO/Si substrate. Clearly, the rectangularity of the *P–E* hysteresis loops for the BFO film can be further improved by inserting a 40-nm-thick buffer layer as shown in Fig. 5b. The remanent polarization (P_r) for the BFO film on 40-nm-thick BNT buffer layer is about 70.2 ± 2 μC/cm^2. This value is found to be greatly enhanced in comparison with that for the $Bi_{3.5}Nd_{0.5}Ti_3O_{12}$ film (~27 μC/cm^2) fabricated on the Pt/Ti/SiO_2/Si(100) substrate [20]. However, further increase of the buffer layer thickness results in the degradation of the rectangularity of the *P–E* hysteresis loops and reduction of the P_r value. Similar phenomena have been observed in trilayered $(Ba_{0.5}Sr_{0.5})TiO_3$/$Pb(Zr_{0.52}Ti_{0.48})O_3$/$(Ba_{0.5}Sr_{0.5})TiO_3$ thin films [21]. As mentioned in the Sect. "Introduction", part of the voltage can be applied on the bottom buffer layer since the buffer layer and BFO layer are in series connection, leading to that the domains in the BFO film cannot be fully switched. However, the dependence of ΔP [$\Delta P = P^*$ (switched polarization) $- P^\wedge$ (nonswitched polarization)] on the electric field (see Fig. 5e) suggests that the effect related to the voltage consumed by the buffer layer is not a dominant factor. Otherwise, the value of ΔP for the BFO film with 160-nm-thick BNT buffer layer would be difficult to become saturated due to the gradual switching of the domains with the increase of electric field. More likely, we ascribe the reduction of the P_r value for the overall double-layered structure to the lower P_r of the BNT buffer layer. Actually, the BFO has a large intrinsic polarization, which is difficult to be obtained due to the severe leakage characteristic. Inserting a thin insulting BNT buffer layer between the BFO film and ITO electrode favors the observation the large polarization of BFO film. However, the P_r value of the BNT buffer layer is very low, which can dilute the total ferroelectric polarization of the overall double-layered structure. That is, with the increase of the BNT buffer layer thickness, this effect will become stronger and result in the gradual reduction of the P_r value. Generally, in the double-layered thin films, the charge-retaining ability should be partially degraded with the increase of the buffer layer thickness due to the domain backswitching during the delay time [22, 23]. This hypothesis can be confirmed by the retention measurements as discussed below.

To further evaluate the stability of the polar state for the double-layered films, a normalized ΔP as a function of the retention time for all films is illustrated in Fig. 5f. The reductions of ΔP within 10^4 s at room temperature are about 0.46%, 4.8%, 8.3%, and 12.5% for BFO films with 0-, 40-, 80-, 160-nm-thick BNT buffer layer. The BFO film with thinner BNT buffer layer exhibits better charge-retaining ability, which makes it a promising candidate for the charge storage or memory devices.

Conclusion

To summarize, BFO films deposited on various thicknesses (0, 40, 80, and 160 nm) of BNT buffer layers were successfully fabricated on ITO/Si substrates using a metal organic decomposition process. The BNT buffer layers were demonstrated to be effective in facilitating the formation of (110)-oriented grains and reducing the leakage current densities in BFO films. Accordingly, well saturated *P–E* hysteresis loops can be obtained in the BFO films with BNT buffer layers compared with that in the BFO film deposited directly on ITO/Si substrate. The BFO film with thinner BNT buffer layer exhibits larger remnant polarization, better rectangularity of *P–E* hysteresis loops, as well as better charge-retaining ability. The above results indicate that 40-nm-thick BNT buffer layer is enough for reducing the leakage current of BFO film without sacrificing its ferroelectric properties.

Acknowledgements This work was supported by funding from the National Natural Science Foundation of China (90207025 and 50502016) and the National Science Foundation of Shandong Province (Z2004G06).

References

1. Kiselev SV, Ozerov RP, Zhdanov GS (1963) Sov Phys Dokl 7:742
2. Teague JR, Gerson R, James WJ (1970) Solid State Commun 8:1073
3. Smolenskii GA, Chupis I (1982) Sov Phys Usp 25:475
4. Kubel F, Schmid H (1990) Acta Crystallogr B 46:698
5. Eerenstein W, Morrison FD, Dho J, Blamire MG, Scott JF, Mathur ND (2005) Science 307:1203a
6. Shvartsman VV, Kleemann W, Haumont R, Kreisel J (2007) Appl Phys Lett 90:172115
7. Lebeugle D, Colson D, Forget A, Viret M (2007) Appl Phys Lett 91:022907
8. Qi X, Tsai PC, Chen YC, Ko CH, Huang JCA, Chen IG (2008) J Phys D 41:232001
9. Hu GD, Cheng X, Wu WB, Yang CH (2007) Appl Phys Lett 91:232909
10. Uchida H, Ueno R, Funakubo H, Koda S (2006) J Appl Phys 100:014106
11. Singh SK, Ishiwara H, Maruyama K (2006) Appl Phys Lett 88:262908
12. Kim JK, Kim SS, Kim W, Bhalla AS, Guo R (2006) Appl Phys Lett 88:132901
13. Li YW, Sun JL, Chen J, Meng XJ, Chu JH (2005) Appl Phys Lett 87:182902
14. Cheng Z, Wang X, Kannan CV, Ozawa K, Kimura H, Nishida T, Zhang S, Shrout TR (2006) Appl Phys Lett 88:132909
15. Huang F, Lu X, Lin W, Cai W, Wu X, Kan Y, Sang H, Zhu J (2007) Appl Phys Lett 90:252903
16. Qi YJ, Lu CJ, Zhang QF, Wang LH, Chen F, Cheng CS, Liu BT (2008) J Phys D 41:065407
17. Liu HR, Wang XZ (2008) J Phys D 41:175411
18. Chen XM, Hu GD, Yan J, Wang X, Yang CH, Wu WB (2008) J Phys D 41:225402
19. Hu GD (2006) J Appl Phys 100:096109
20. Zhong XL, Wang JB, Zheng XL, Zhou YC (2004) Appl Phys Lett 85:5661
21. Yan F, Wang Y, Chan HLW, Choy CL (2003) Appl Phys Lett 82:4325
22. Lee CC, Wu JM, Hsiung CP (2007) Appl Phys Lett 90:182909
23. Cui SG, Hu GD, Wu WB, Yang CH, Jiao LL, Wen Z (2009) J Am Ceram Soc. doi:10.1111/j.1551-2916.2009.03051.x